Available online at www.sciencedirect.com
ScienceDirect
Journal of the European Ceramic Society 31 (2011) 605–609
www.elsevier.com/locate/jeurceramsoc

Effects of pore size and orientation on dielectric and piezoelectric properties of 1–3 type porous PZT ceramics

Rui Guo, Chang-An Wang *, AnKun Yang

State Key Lab of New Ceramics and Fine Processing, Department of Materials Science and Engineering, Tsinghua University, Beijing 100084, PR China

Received 14 July 2010; received in revised form 5 October 2010; accepted 11 October 2010
Available online 23 November 2010

Abstract

Porous PZT ceramics have drawn an increasing amount of interest in recent years due to their superior properties compared with the dense material. However, researchers have usually dedicated effort to 0–3 and 3–3 type porous PZT ceramics and little attention has been focused on 1–3 type. The 1–3 type porous PZT ceramics with high porosity were fabricated in this study by freeze-casting process. All samples possessed high piezoelectric coefficient (d_{33}) with high porosity owing to the special one-dimensional ordered porous structure along the poling direction. The d_{33} values increased by either improving the pore channel orientation level or decreasing pore size. The relative permittivity improved only with the enhancement of pore channel orientation level. The acoustic impedances ranged from 1.45 to 1.35 MRayls which could match well with those of biological tissue or water; therefore, this material would be beneficial in hydrophone applications.

Keywords: Freeze-casting; Porosity; Piezoelectric properties; PZT

1. Introduction

Porous lead zirconate titanate (PZT) ceramics have drawn an increasing amount of interest due to their low density, high hydrostatic figure of merit and low acoustic impedance (*Z*). A variety of manufacturing methods are available for the production of porous piezoelectric ceramics, including the BURPS (Burned out Polymer Spheres),[1–3] the solid freeform fabrication (SFF),[4] the fused deposition,[5] gel-casting[6] and freeze casting (or freeze drying)[7,8] processes. Each preparation technique results in distinct microstructure, such as pore size, pore morphology, pore connectivity, and pore alignment. The piezoelectric properties of porous PZT ceramics are strongly dependent on their microstructure, especially on pore structure. Based on the association between pores and matrix, it can be divided into 0–3, 1–3 and 3–3 type PZT-air composites (porous PZT ceramics). The first number represents the connectivity of passive air phase and the second is the connectivity of active PZT phase. Researchers have dedicated effort to 0–3 and 3–3 type porous PZT ceramics,[2,9–11] yet little attention has been focused on 1–3 type porous PZT ceramics in these years.

In this study, 1–3 type porous PZT ceramics with one-dimensional ordered pore channel structure were fabricated by freeze-casting technique, and the effects of pore channel orientation level and pore diameter on the dielectric and piezoelectric properties were investigated.

2. Materials and methods

2.1. Materials selection

PZT-5H powder (BaoDing HongSheng Acoustic Electron Apparatus Co., Ltd, China, $d_{33} = 720 \times 10^{-12}$ C/N, $\varepsilon_r = 4360$ (values refer to dense PZT measured at constant (zero) stress by the same impedance bridge as below) with a mean particle size of 1.8 μm and density of 7.6 g/cm^3 was used as ceramic powder. Tert-butyl alcohol (TBA, chemical purity, Beijing Yili Chemical Co., Beijing, China) was chosen for a freezing vehicle. In addition, commercial available polyvinyl butyral (PVB, chemical purity, China) and acacia (chemical purity, China) were used as organic binder and dispersant, respectively.

* Corresponding author. Tel.: +86 10 62785488; fax: +86 10 62785488.
E-mail addresses: wangca@mail.tsinghua.edu.cn, huliangfa@gmail.com (C.-A. Wang).

0955-2219/$ – see front matter © 2010 Elsevier Ltd. All rights reserved.
doi:10.1016/j.jeurceramsoc.2010.10.019

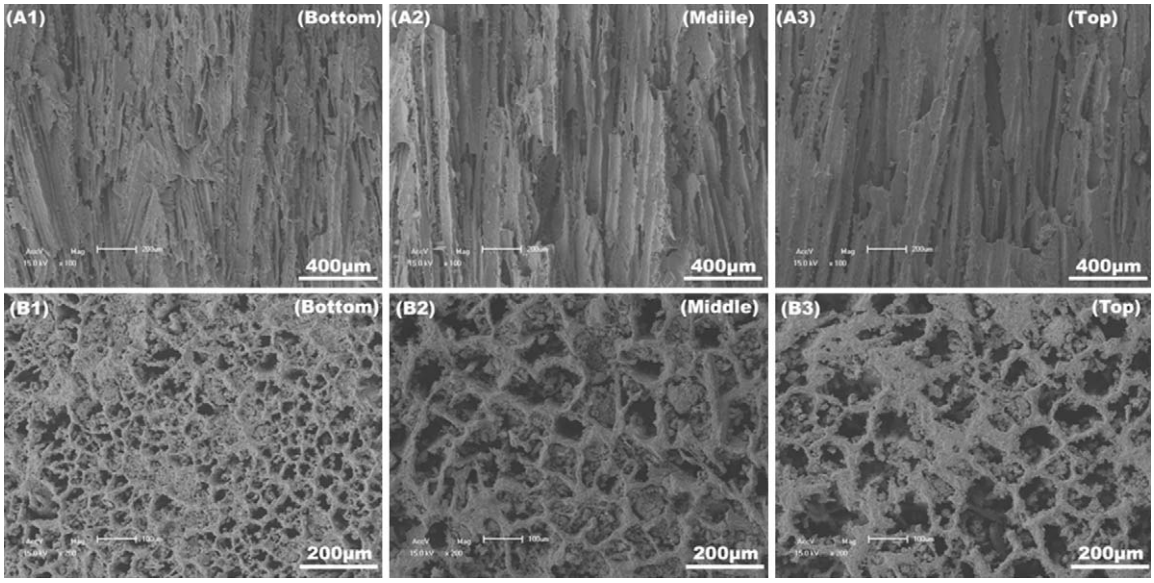

Fig. 1. Fracture surfaces of 1–3 type porous PZT ceramics with different locations. (A1–A3) and (B1–B3) are vertical sections (parallel to the freezing direction) and transverse sections (perpendicular to the freezing direction) for bottom, middle and top section, respectively.

2.2. Sample preparation

A TBA-based slurry with 15 vol% PZT solid loading was prepared by ball milling for 4 h at room temperature, with 1.2 wt% acacia dispersant, 1.2 wt% PVB binder and 1.5 wt% deionized water added (all proportions were based on TBA content). The slurry was de-gassed and cast into a cylindrical polyamide mold, which was affixed to a copper board as its bottom for good heat-conduction. Immediately after casting, the bottom copper face of the mold was immersed in −30 °C chilled alcohol. In this condition, the TBA crystal prisms were induced to grow vertically along the direction from bottom (cold end) to top (hot end), consequently unidirectional pore channels would run through the whole cast body in the same direction. The frozen samples were carefully removed from the molds and then the solidified fugitive phase TBA was sublimated in a freeze-dryer (Type FD-1A-50, Boyikang Corp., Beijing, China) at −50 °C. The green bodies were then sintered in corundum crucibles containing $PbZrO_3$ powder to produce an excess-PbO atmosphere at 1300 °C for 2 h. Then each porous PZT ceramic cylinder (PZT cylinder) was sliced into three sections which was named 'bottom section' (located at cold end), 'middle section' and 'top section', respectively. Each section led to 3–5 samples and all samples were machined and ground to disc shape with 20 mm in diameter and 2 mm in height.

2.3. Characterization

The density and porosity of the sintered samples were measured by using the water displacement method based on the Archimedean principles. The microstructure was observed with scanning electron microscopy (SEM, SHIMAZU SSX-550, Japan). Pore-size distributions were analyzed by a mercury intrusion method (AutoPore IV 9510). For measuring dielectric and piezoelectric properties, electrodes were made by screening a thin silver paste to the surfaces of sample, followed by heat treatment at around 550 °C for 20 min. To minimize its penetration into ceramic bodies, the silver paste was made highly viscous. Subsequently, the samples were poled in a silicone oil bath at 120 °C by applying a DC field of 1 kV/mm (where as 2 kV/mm for dense PZT ceramics in this study. The different applied poling fields used for dense and 1–3 type porous PZT ceramics were based on our experiment results and were chosen to allow the samples to be fully polarized without being damaged at the same time) for 25 min, and were then aged for 24 h before testing. The longitude piezoelectric coefficient (d_{33}) was measured by a piezo-meter system (Piezo Test, UK). Spectrum characteristics (f_r, the resonant vibration frequency) and permittivity (ε_r) were measured under constant (zero) stress by using an impedance bridge (HP-4194A).

3. Results and discussion

3.1. Microstructure

The images of Fig. 1(A1)–(A3) are for typical vertical sections that parallel to the solidification direction. It reveals that the pore channels of all samples were highly aligned along the freezing direction but small differences could be seen of the sample at the different locations. The orientation level of the one at bottom location was the worst in all samples which was caused by the crystal nucleation process of TBA while the top location was inferior which could be ascribed the overgrowth of the prisms of TBA crystals caused by the lower temperature gradient. The pore channel orientation of the middle part was the best in that the appropriate temperature gradient and moderate distance away from the crystal nucleation area. The images of Fig. 1(B1)–(B3) are for transverse sections that perpendicular

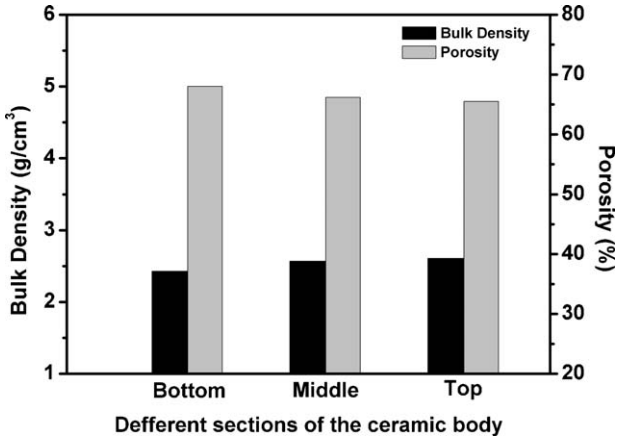

Fig. 2. Porosity and bulk density of samples located at different position of the 1–3 type porous PZT ceramic body.

to the freezing direction. The pore size ranged around dozens of micrometers in diameter, which were in good agreement with the below mercury intrusion results.

3.2. Porosity and pore-size distribution

Fig. 2 shows the porosity and bulk density of samples located at different position of the 1–3 type porous PZT cylinders. The porosities (bulk density) were 68.0% (2.43 g/cm^3), 66.2% (2.57 g/cm^3) and 65.5% (2.61 g/cm^3) for bottom section, middle section and top section, respectively. It was obvious that the porosity and density of all samples shared very small difference because all the PZT cylindered were fabricated with the same 15 vol% solid loading slurry which had good mobility and uniformity.

Fig. 3 reveals that the pore size distribution of all the three parts of 1–3 type porous PZT ceramic cylinders. The pore size distribution exhibited a unimodal distribution, but peak location varied significantly with different positions. The median pore diameters were 26.09 μm, 40.96 μm and 53.57 μm for bottom part (cold end), middle part and top part, respectively. The pore channels of the porous PZT ceramics became larger and larger with position away from the cold end. The pore channels of the top part were twice as broad as those of the bottom part.

During the directional freeze casting process of the slurry, the bottom of mold was fixed on a copper plate which was controlled at −30 °C whereas the top part of the slurry was initially at room-temperature in the beginning. The crystal nucleuses of TBA were first formed at cold end and then grew upward from this region. The different environmental temperature created different temperature gradient in the slurry. Correspondingly, the temperature gradient decreased as the solidification front moved away from the cooling copper plate surface. This would allow continued overgrowth of the prisms of TBA crystals and the size of the prisms would be expected to increase with distance from the cold end. Since the pore channels were formed as a replica of the TBA crystal prisms, the pore channels of upper part were certainly broader when the distance was farther away from the bottom.

3.3. Piezoelectric property

As seen from Fig. 4, the piezoelectric d_{33} coefficients were 589 pC/N, 675 pC/N and 623 pC/N for the top, middle and bottom section, respectively. All samples from different locations remained high piezoelectric coefficient (from 81.8% to 93.0% to that of the dense PZT ceramics) although the porosity was over 65%. This should be ascribed to the one-dimensional ordered pore channel structure which made the porous PZT ceramics 1–3 type PZT-air composites. The piezoelectric coefficient of 1–3 type porous PZT ceramics can be calculated by the parallel-mixture rule[12]:

$$d_{33}^{1-3} = \frac{f_{PZT} d_{33}^{PZT} S_{33}^{air}}{f_{PZT} S_{33}^{air} + (1 - f_{PZT}) S_{33}^{PZT}} \quad (1)$$

where d_{33}^{1-3} is piezoelectric coefficient of the 1–3 type porous PZT ceramic, f_{PZT} is the volume fraction of PZT phase, d_{33}^{PZT} is the piezoelectric coefficient of dense PZT ceramics, S_{33}^{air} and S_{33}^{PZT} are elastic compliances of air and PZT, respectively. Elas-

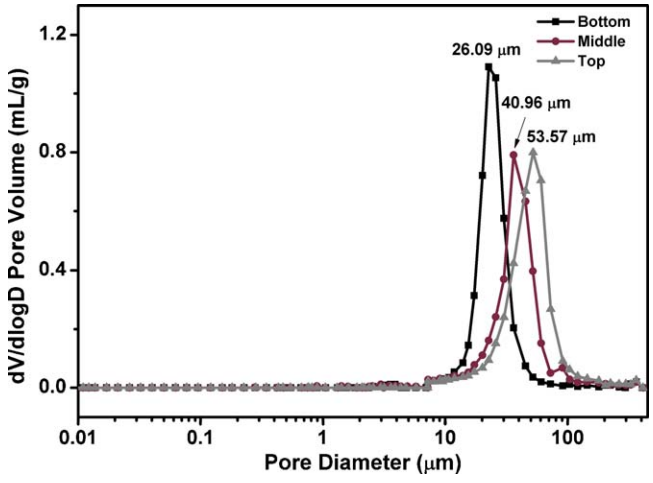

Fig. 3. Pore size distribution of samples from different sections of the 1–3 type porous PZT ceramics.

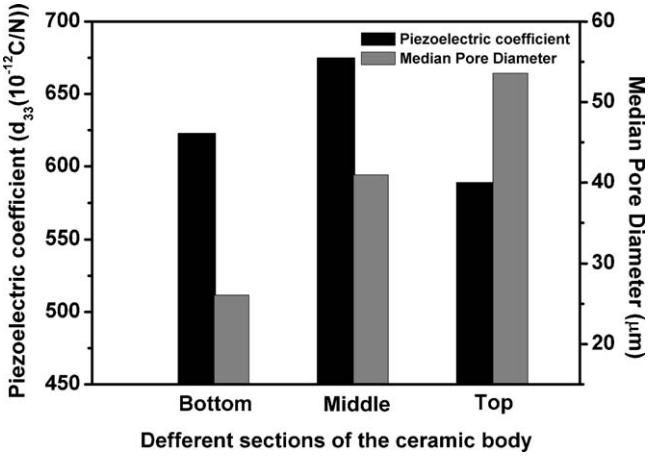

Fig. 4. Piezoelectric coefficients and median pore diameters of 1–3 type porous PZT ceramics with different locations.

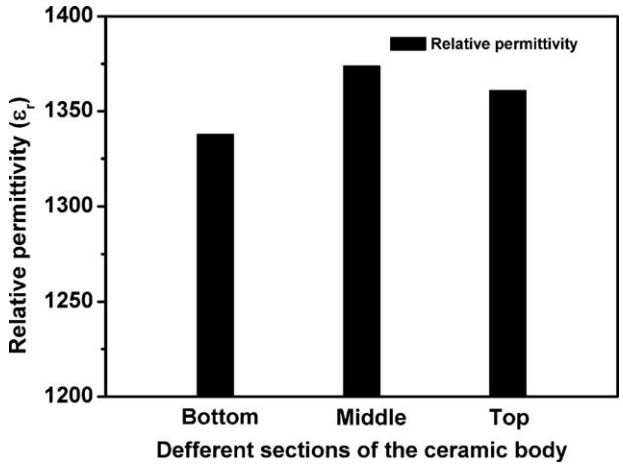

Fig. 5. Relative permittivity at 1 kHz of the 1–3 type porous PZT ceramics at different locations.

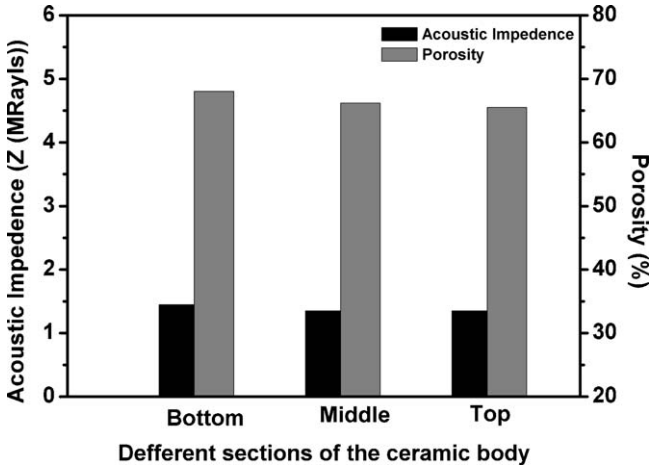

Fig. 6. Acoustic impedance and porosity of 1–3 type porous PZT ceramics at different locations.

tic compliance represents the deformation ability of material, $S_{33}^{PZT} = 1.87 \times 10^{-11}$ m^2/N is assumed[13] and S_{33}^{air} approaches to infinity. It is obvious that 1–3 type porous PZT ceramics should have the same piezoelectric coefficient as dense PZT ceramics according to Eq. (1).

However, Fig. 4 shows that the d_{33}^{1-3} values were lower than expected by theory. This might be owing to the minute amount of defects such as tenuous holes between particles on ceramic walls that emerged due to the very low solid loading and high porosity. In that case, the structures of porous PZT ceramics would deviate slightly from the exact 1–3 type to 3–3 type and at the same time the defects could also influence degree of poling during the polarization so the defects could lead to the decreasing of piezoelectric coefficient. On the other hand, the inferior orientation of the pore channels can also made the porous structure departed from 1–3 type to 3–3 type; so consistent with Fig. 1, we obtained the highest piezoelectric coefficient in the middle part due to the superior orientation. It should also be mentioned that the top part possessed better orientation level while presented inferior piezoelectric property than the bottom one even though they had the same porosity level. The reason might be attributed to the distinct difference between the pore diameters of these two parts. As can be seen from Figs. 1, 3 and 4, the pore diameter of the bottom part was much smaller than that of the top part. Generally, with certain porosity, a sample with small pores has more total pore surface and thus more grain-pore contact area, which provides more relaxation chance for stress caused by the movement of domain walls.[14] In this sense, samples with small pores are more promising to enhance the mobility of domain walls and hence the piezoelectric coefficient had superior performance as indicated by Fig. 4.

3.4. Relative permittivity

According to previous research,[16] the alignment of pores in the direction of poling resulted in an increase in the volume fraction of active material connected in the poling-direction that would result in an increase in ε_r, whereas pore shape did not greatly affect ε_r. As Fig. 5 shows, the relative permittivity was 1338, 1374, and 1361 for the bottom, middle and top parts, respectively. The permittivity of the dense PZT ceramics was 4360 in this study. All samples presented much higher ε_r at 1 kHz frequency than those of other type's porous PZT ceramics in our former research even with the same porosity.[15] This is mainly due to the special one-dimensional ordered pore structure. The permittivity decreased from 1374 of the middle part to 1361 of the top one and then to 1338 of the bottom one which well coincided with the orientation level of the different location that showed in Fig. 1 no matter what the pore diameters were.

3.5. Acoustic impedance

Hydrophones or medical imaging devices usually require ultrasound transmission into water or tissue, whereas a huge difference in acoustic impedances exists between PZT ceramics (>10 MRayls, ~16 MRayls in this study) and human tissue (1–2 MRayls) or water (~1.5 MRayls). Porous PZT ceramics provide a solution to this problem by decreasing density and introducing porosity, the passive phase, into materials.

The acoustic impedance was calculated by:

$$Z = \rho D f_r \quad (2)$$

where ρ is measured density, D is the diameter and f_r is the resonant vibration frequency of samples. As shown in Fig. 6, the acoustic impedances were all at the same level ranged from 1.45 to 1.35, matching well with those of biological tissue and water, which would be beneficial in improving acoustic matching by minimizing energy loss at the interface of the ceramic and medium. This result is much lower than our former research (porosity = 58.6%, Z = 3.0 MRayls)[6,13] which was might due to the higher porosity and special one-dimensional ordered pore structure along the propagation direction of acoustic wave.

4. Conclusion

The 1–3 type porous PZT ceramics with one-dimensional ordered pore channel structure were fabricated by TBA-based directional freeze-casting process. The porosity was higher than

65%, whereas all samples possessed high piezoelectric coefficient (d_{33}) and high relative permittivity due to the special pore structure. Superior pore channel orientation contributed to the improvement of both piezoelectric coefficient (d_{33}) and higher relative permittivity, yet smaller pore diameters only enhanced the piezoelectric property but had no obvious influence on permittivity. The acoustic impendence was sensitive to the porosity and special one-dimensional ordered pore structure but showed no obvious response to the variation of pore diameters. The acoustic impedances were ranged from 1.45 to 1.35 in this study which could match well with that of biological tissue and water.

Acknowledgements

This work was financially supported by the National Natural Science Foundation of China (Grant No.: 50921061), the Natural High Technology Research and Development Program of China ("863" Program, Grant No.: 2007AA03Z435) and State Key Development Program of Basic Research of China ("973" program, Grant No.: 2006CB605207-2).

References

1. Zeng T, Dong XL, Mao CL, Zhou ZY, Yang H. Effects of pore shape and porosity on the properties of porous PZT 95/5 ceramics. *J Eur Ceram Soc* 2007;**27**:2025–9.
2. Li JF, Takagi K, Ono M, Pan W, Watanabe R, Almajid A, et al. Fabrication and evaluation of porous piezoelectric ceramics and porosity-graded piezoelectric actuators. *J Am Ceram Soc* 2003;**86**:1094–8.
3. Bowen CR, Perry A, Lewis A, Kara H. Processing and properties of porous piezoelectric materials with high hydrostatic figures of merit. *J Eur Ceram Soc* 2004;**24**:541–5.
4. Safari A, Allahverdi M, Akdogan EK. Solid freeform fabrication of piezoelectric sensors and actuators. *J Mater Sci* 2006;**41**:177–98.
5. Allahverdi M, Danforth SC, Jafari M, Safari A. Processing of advanced electroceramic components by fused deposition technique. *J Eur Ceram Soc* 2001;**21**:1485–90.
6. Yang A, Wang CA, Guo R, Huang Y, Nan CW. Porous PZT ceramics with high hydrostatic figure of merit and low acoustic impedance by TBA-based gel-casting process. *J Am Ceram Soc* 2010;**93**:1427–31.
7. Lee S, Jun S, Kim H, Koh Y. Fabrication of porous PZT-PZN piezoelectric ceramics with high hydrostatic figure of merits using camphene-based freeze casting. *J Am Ceram Soc* 2007;**90**:2807–13.
8. Pekor CM, Kisa P, Nettleship I. Effect of polyethylene glycol on the microstructure of freeze-cast alumina. *J Am Ceram Soc* 2008;**91**:3185–90.
9. Roncari E, Galassi C, Craciun F, Capiani C, Piancastelli A. A microstructural study of porous piezoelectric ceramics obtained by different methods. *J Eur Ceram Soc* 2001;**21**:409–17.
10. Praveenkumar B, Kumar HH, Kharat DK. Study on microstructure, piezoelectric and dielectric properties of 3–3 porous PZT composites. *J Mater Sci-Mater Electron* 2006;**17**:515–8.
11. Bowen CR, Topolov VYu. Piezoelectric sensitivity of $PbTiO_3$-based ceramic/polymer composites with 0–3 and 3–3 connectivity. *Acta Mater* 2003;**51**:4965–76.
12. Shi Z, Nan CW, Zhang J. Magnetoelectric properties of multiferroic composites with pseudo-1–3-type structure. *J Appl Phys* 2006;**99**:124108.
13. Nan CW. Effective-medium theory of piezoelectric composites. *J Appl Phys* 1994;**76**:1155–63.
14. Yang AK, Wang CA, Guo R, Huang Y. Microstructure and electrical properties of porous PZT ceramics fabricated by different methods. *J Am Ceram Soc* 2010;**93**:1984–90.
15. Yang AK, Wang CA, Guo R, Huang Y, Nan CW. Effects of sintering behavior on microstructure and piezoelectric properties of porous PZT ceramics. *Ceram Int* 2010;**36**:549–54.
16. Bowen C, Kara H. Pore anisotropy in 3–3 piezoelectric composites. *Mater Chem Phys* 2002;**75**:45–9.